Mechanical Systems and Signal Processing 135 (2020) 106443

Contents lists available at ScienceDirect

Mechanical Systems and Signal Processing

journal homepage: www.elsevier.com/locate/ymssp

Fault diagnosis of rotating machines based on the EMD manifold

Jun Wang [a,d], Guifu Du [b], Zhongkui Zhu [b], Changqing Shen [b], Qingbo He [c,*]

[a] School of Computer Science and Technology, Soochow University, Suzhou, Jiangsu 215006, PR China
[b] School of Rail Transportation, Soochow University, Suzhou, Jiangsu 215131, PR China
[c] State Key Laboratory of Mechanical System and Vibration, Shanghai Jiao Tong University, Shanghai 200240, PR China
[d] Jiangsu KTK Locomotive & Rolling Stock Co., Ltd., Changzhou, Jiangsu 213164, PR China

ARTICLE INFO

Article history:
Received 1 June 2019
Received in revised form 25 September 2019
Accepted 14 October 2019
Available online 23 October 2019

Keywords:
Empirical mode decomposition
Manifold learning
Machinery fault diagnosis
Noise assistance
Time-frequency signal decomposition

ABSTRACT

One challenge of the existing noise-assisted methods for solution of mode mixing problem of empirical mode decomposition (EMD) is that, the decomposed modes contain much residual noise derived from both added and self-contained noise. This paper proposes a new noise-assisted method, called EMD manifold (EMDM), for enhanced fault diagnosis of rotating machines. The major contribution is that the new method nonlinearly and adaptively fuses the fault-related modes containing different noise via a manifold learning algorithm, by which true fault-related transients are preserved, while fault-unrelated components including mode-mixing-induced components and the residual noise derived from both the added and self-contained noise are greatly suppressed. First, the sensitive mode is located among the modes obtained by the EMD method according to a newly proposed criterion. Then, a high-dimensional matrix is constructed of the sensitive modes obtained through a small number of EMD trials on the signals plus noise of different amplitudes. Finally, the manifold learning algorithm is performed on the high-dimensional matrix to extract intrinsic manifold of the fault-related transients. The high-dimensional matrix is repeatedly constructed with random noise added to adjust local data distribution of the matrix for adaptive EMDM feature learning. Experimental studies on gearbox and bearing faults are conducted to validate the proposed method and its enhanced performance over traditional noise-assisted EMD methods.

1. Introduction

Rotating machines are widely used in modern manufacturing, aerospace, transportation vehicles, wind turbines, etc. The key components of the rotating machines, especially bearings and gears, are prone to damage due to long term running under harsh working conditions. Continuous attentions have been paid to fault diagnosis of the rotating machines both in academia and industry so as to guarantee safety, reliability, stability of the machines and reduce economic losses caused by unexpected machine breakdown. Tremendous fault diagnostic techniques based on vibration signal analysis have been proposed during the past a few decades, which can be categorized into signal processing methods [1–4], intelligent diagnostic methods [5–7] and remaining useful life predicting methods [8–10]. The signal processing methods intend to remove

* Corresponding author.
E-mail address: qbhe@sjtu.edu.cn (Q. He).

https://doi.org/10.1016/j.ymssp.2019.106443
0888-3270/

noise involved in the measured vibration signals and extract features that would facilitate fault identification and, therefore, are essential for effective fault diagnosis of the rotating machines.

Empirical mode decomposition (EMD) is a well-known time–frequency signal decomposition tool that is useful for analyzing nonstationary and nonlinear signals, and has been widely applied to the field of machinery fault diagnosis as a signal processing method [11–13]. A small number of complete and nearly orthogonal components called intrinsic mode functions (IMFs) are adaptively obtained via the EMD based on local characteristic time scales of the analyzed signal [14]. Since the oscillatory mode of a rotating machine with a localized fault satisfies the requirements of the IMF, the amplitude modulation and/or frequency modulation (AM-FM) component resulted from the fault is supposed to be extracted from the measured vibration signal by using the EMD. However, the AM-FM component usually exhibits as repetitive transients in the vibration signal, which is intermittent and could yield one of the major drawbacks of the EMD, i.e. mode mixing problem. The mode mixing is defined as mergence of the components with dramatically disparate scales into one IMF and/or separation of a similar scale component into different IMFs. Suffering from the problem of mode mixing, the fault-related IMFs extracted still contain some fault-unrelated components and noise, which hinders the accurate identification of fault information.

Currently, there are generally two strategies to alleviate the mode mixing problem of the EMD. One is to mix the original signal with some masking signals [15]. However, since the masking signal depends on the component being extracted, the design of appropriate masking signal is a challenging task [16]. The other strategy is to add noise to the investigated signal, which was first discovered by Wu and Huang [17] in the method named ensemble empirical mode decomposition (EEMD). The EEMD is a noise-assisted method that utilizes the full advantage of the statistical characteristics of white noise to populate the whole time–frequency space uniformly with the constituting components of different scales. The components of different scales in this uniform reference frame will be projected onto proper IMFs in the EEMD method. The EEMD represents a major improvement over the original EMD in terms of mode mixing problem and has been applied to machinery fault diagnosis as a more mature version [18–20]. Nevertheless, the introduction of white noise to the analyzed signal gives rise to some new problems, including the determination of proper values of noise amplitude and ensemble number, and the removal of added noise, which remain to be open questions and have attracted the interest of some researchers for further improvement.

The noise amplitude and ensemble number are two crucial parameters that affect the decomposing performance of the EEMD. The effect of adding white noise is to homogenize the extrema distribution of the original signal for alleviating the mode mixing problem. If the noise amplitude is too small, the noise may not cause enough change of extrema distribution of the original signal. As a result, the mode mixing will not be alleviated effectively. On the other hand, if the noise amplitude is too large, the noise retaining in the assembled modes would be considerably large with a limited ensemble number. A large ensemble number would decrease the residual noise in the obtained modes. Therefore, the set of ensemble number is based on error tolerance of the decomposing results, and generally requires a few hundred for good results. Empirical and fixed values of the two parameters were suggested in the original EEMD [17], but are not always applicable for different signals. Therefore, some methods aiming at determining the parameters adaptive to the signals have been proposed. Lei et al. [18] designed a kind of noise whose amplitude changes with the signal frequency components during the decomposition process. Chen et al. [21] determined the noise amplitude and ensemble number according to the amplitude of high frequency component contained in the analyzed signal. Besides, optimal noise amplitudes in the EEMD were determined according to the decomposing performance evaluated by some indexes, e.g., correlation measure between the decomposed IMFs and the components in the original signal [22], relative root-mean-square error (RRMSE) defined in [23], Pearson coefficient of the correlation between the successive IMFs [24]. Nevertheless, the computational burden is heavy in these methods because the results corresponding to a set of parameters have to be obtained.

The added noise is useful for mode mixing alleviation, while is annoying if not removed eventually. A lower noise level in the reconstructed signal can be achieved with a larger ensemble number in the EEMD method, however, at the cost of a lower computational efficiency. Some new techniques with respect to reducing the residual noise in the reconstructed signal for the noise-assisted methods have been achieved in recent years. Yeh et al. [25] proposed a complementary ensemble empirical mode decomposition (CEEMD) method to reduce the residual noise in the reconstructed signal with a less ensemble number by adding positive and negative white noise in pairs. Xue et al. [26] proposed to add only one pair high-frequency white noise with positive and negative signs to the original signal for more efficient treatment of the residual noise in the reconstructed signal. Zheng [27] believed that the last several IMFs obtained by the EMD have no mode mixing problem, based on which only the first several IMFs mainly containing intermittency or noise components were extracted in the ensemble way of the CEEMD. Less noise retained in the reconstructed signal and much costing time was saved in this method as compared to the EEMD and CEEMD. Torres et al. [28] found that different realizations of signal plus noise may produce different number of modes in the EEMD method. They added a particular noise at each stage of the decomposition and computed a unique residue to obtain each mode, which guarantees the completeness of the decomposition and achieves a numerically negligible reconstruction error with a smaller ensemble size. This method is termed complete ensemble empirical mode decomposition with adaptive noise (CEEMDAN). All the methods stated above aim to remove the noise added as much as possible in the signal reconstruction procedure. However, it is the true IMFs that should be focused on in the signal decomposition methods; it would be more significant to reduce the residual noise contained in the obtained IMFs than that contained in the reconstructed signal. To reach this goal, an improved CEEMDAN was proposed by defining the true mode as the difference between the current residue and the average of the local means of the current residue plus particular noise [29]. Less amount of noise contained in the obtained modes was claimed to be achieved in the improved

CEEMDAN as compared to the original CEEMDAN. When analyzing the vibration signals of rotating machines utilizing the EEMD and its variations, in addition to the residual noise added, the fault-related repetitive transients extracted are contaminated by the residual noise involved when measuring the vibration signals. Therefore, the removal of self-contained noise retaining in the fault-related modes obtained by the noise-assisted EMD methods is of great importance in machinery fault diagnosis, which, however, has not been tackled in the existing literature.

This paper intends to remove the residual noise contained in the fault-related modes derived from both the added noise and the self-contained noise for clear identification of the fault-related transients. A new method, termed EMD manifold (EMDM), is proposed for enhanced fault diagnosis of rotating machines. The fault-related IMFs obtained via conducting the EMD on a few signals plus white noise are fused adaptively by a manifold learning algorithm in the new method, instead of being averaged in the methods of EEMD and its variations. Furthermore, the noise amplitudes for different EMD trials vary among a range rather than being fixed values. Thus, there is no need to optimize the noise amplitude in the EMDM. Manifold learning is an effective nonlinear dimensionality reduction method and has been proved to be capable of extracting intrinsic dynamic features related to the nature of different machine faults from high-dimensional data [30–32]. In this paper, a high-dimensional data, called sensitive mode matrix (SMM), are constructed of the fault-related IMFs obtained through a small number of EMD trials with different noise amplitudes. It is conceivable that the oscillatory modes of the IMFs in the SMM behave slightly different because of the possible mode mixing phenomenon and the different amounts of residual noise. However, the transients resulted from the machine fault are fixed structure in every IMF that can be regarded as an underlying manifold of the high-dimensional data, which will be reserved by the manifold learning method. On the other hand, the components involved when mode mixing occurs and the residual noise derived from both added and self-contained noise vary among all the IMFs in the SMM, and will be excluded in the results. Therefore, the fused IMF via the EMDM can reveal the inherent impulsive structure of the fault-related transients, hence the performance of machinery fault diagnosis is enhanced as compared to the EEMD and its variations.

The remainder of this paper is organized as follows. Section 2 briefly reviews the algorithms of EMD and EEMD. Section 3 depicts the details of the proposed EMDM method for the extraction of true fault-related transients of rotating machines. The enhanced performance of the proposed method over the state-of-the-art methods is confirmed by experimental results in Section 4. Section 5 concludes the paper.

2. Reviews of EMD and EEMD

2.1. EMD

EMD is a data-driven, self-adaptive method, by which a multicomponent signal can be decomposed into a set of IMFs. An IMF is the function that fulfills the following conditions: (i) within the whole data set, the number of extrema (local maxima and minima) and that of zero crossings must either equal or differ at most by one, and (ii) at any point, the mean value of the two envelopes estimated by local maxima and local minima is zero. Given a signal $x(t)$, the procedure to decompose it into IMFs is described as follows.

1) Set $k = 0$, $r_k(t) = x(t)$.
2) Find all the local extrema of $r_k(t)$.
3) Construct the upper envelope $e_{\max}(t)$ and lower envelope $e_{\min}(t)$ by interpolating the local maxima and local minima, respectively, via the cubic spline curve fitting.
4) Compute the mean envelope by

$$m(t) = [e_{\max}(t) + e_{\min}(t)]/2. \tag{1}$$

5) Compute the IMF candidate by

$$d_k(t) = r_k(t) - m(t). \tag{2}$$

6) Is $d_k(t)$ an IMF?
   a) No. Set $r_k(t) = d_k(t)$. Repeat steps 2)–6).
   b) Yes. Save the obtained IMF as $c_{k+1}(t) = d_k(t)$. Compute the residue by

$$r_{k+1}(t) = x(t) - \sum_{i=1}^{k+1} c_i(t). \tag{3}$$

7) Set $k = k + 1$. Repeat steps 2)–6) until the final residue $r_K(t)$ becomes a monotonic function.

Finally, K IMFs $c_i(t)$ ($i = 1, 2, \ldots, K$) and one residue $r_K(t)$ are obtained via the EMD. The original signal can be reconstructed by the sum of all the IMFs and the residue as

$$x(t) = \sum_{i=1}^{K} c_i(t) + r_K(t). \tag{4}$$

To illustrate the performance of the EMD on transient feature extraction of a localized fault of rotating machines, a simulated signal including the components of fault-related transients, a sine wave and brown noise is constructed, as shown in Fig. 1. The brown noise is added to mimic the self-contained noise produced when measuring the vibration signal under industrial environment, which has more energy at lower frequencies. By using the EMD to decompose the simulated signal, the first three IMFs are displayed in Fig. 2. It is obvious that the sine wave is split into the three IMFs c_1, c_2 and c_3. The transient component is contained in the first IMF c_1, but is contaminated by part of the sine wave (marked by red ellipses) and the noise between the transients. The result indicates that the mode mixing problem may occur in the IMFs obtained by the EMD method and may not be solved by the self-contained brown noise. Furthermore, the self-contained noise may reside in the extracted IMFs. The component involved when mode mixing occurs and the residual noise derived from the self-contained noise are expected to be removed for clear identification of the fault-related transients.

2.2. EEMD

The EEMD was proposed aiming at eliminating the mode mixing problem with the assistance of added white noise. A number of EMD trials are performed on the analyzed signal plus different white noise with finite amplitude. The ensemble means of the corresponding IMFs generated from all the trials are defined as the true IMFs in the EEMD. The EEMD algorithm for a given signal $x(t)$ can be described as follows.

1) Generate *Ne* signals plus noise by

$$x_l(t) = x(t) + \beta x_{std} n_l(t), \ l = 1, 2, \ldots, Ne \tag{5}$$

where $n_l(t)$ is a zero-mean unit-variance white noise for the lth trial, x_{std} is the standard deviation of $x(t)$, and β is the ratio of the standard deviation of the noise to x_{std}.

2) Decompose the noise-added signal series $\{x_l(t)\}$ (l = 1, 2, ..., *Ne*) separately using the EMD method described in Section 2.1. A series of IMFs $\{c_{l,i}(t)\}$ (l = 1, 2, ..., *Ne* and i = 1, 2, ..., K) are obtained, where $c_{l,i}(t)$ means the ith IMF of the lth EMD trial.
3) Average the corresponding IMFs obtained in the *Ne* EMD trials to obtain the true IMFs by

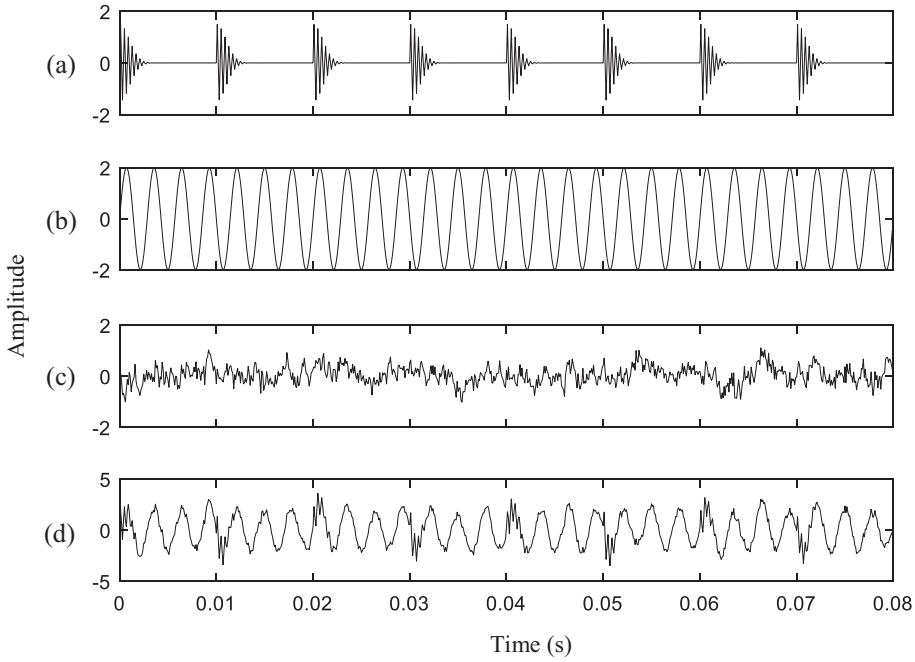

Fig. 1. The simulated signal: (a) component of fault-related transients; (b) component of a sine wave; (c) brown noise component; (d) the simulated signal produced by mixing (a)–(c).

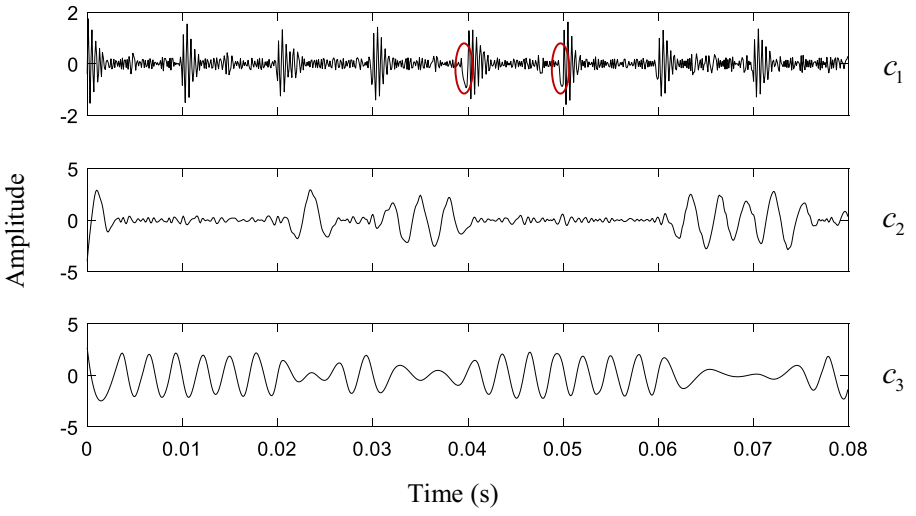

Fig. 2. The first three IMFs of the simulated signal using the EMD.

$$\bar{c}_i(t) = \frac{1}{Ne}\sum_{l=1}^{Ne} c_{l,i}(t),\ i = 1, 2, \ldots, K \tag{6}$$

The EEMD algorithm described above is applied to analyze the simulated signal shown in Fig. 1(d). The ensemble number is set as $Ne = 100$. Three different amplitudes of the added noise are adopted by setting $\beta = 0.01$, 0.2 and 1 successively. The three results including the first a few IMFs are plotted in Figs. 3–5, respectively. In Fig. 3, the three IMFs have little difference from those in Fig. 2 because the added noise with $\beta = 0.01$ is too small to change the extrema distribution of the signal for solving the mode mixing problem. In Fig. 4, it is clear that the two components included in the simulated signal are well decomposed into two IMFs with $\beta = 0.2$; the IMF $\bar{c}_1$ is the fault-related transients and the IMF $\bar{c}_3$ is the sine wave, indicating that the mode mixing problem is alleviated. Some random noise is separated into the IMF $\bar{c}_2$. However, some noise still distributes among the transients of $\bar{c}_1$. The noise in $\bar{c}_1$ comes from the self-contained noise and the added noise as well. With the increase of the added noise level, the level of residual noise contained in the first IMF $\bar{c}_1$ increases, as illustrated in Fig. 5 with $\beta = 1$. The sine wave component is removed from $\bar{c}_1$ in Fig. 5, but is split into $\bar{c}_3$ and $\bar{c}_4$. Thus, the mode mixing problem is not well solved with large noise. These results demonstrate that proper parameters require to be set for the EEMD to solve the mode mixing problem, and the residual noise among the fault-related transients of rotating machines is unable to be removed by the average procedure of the EEMD.

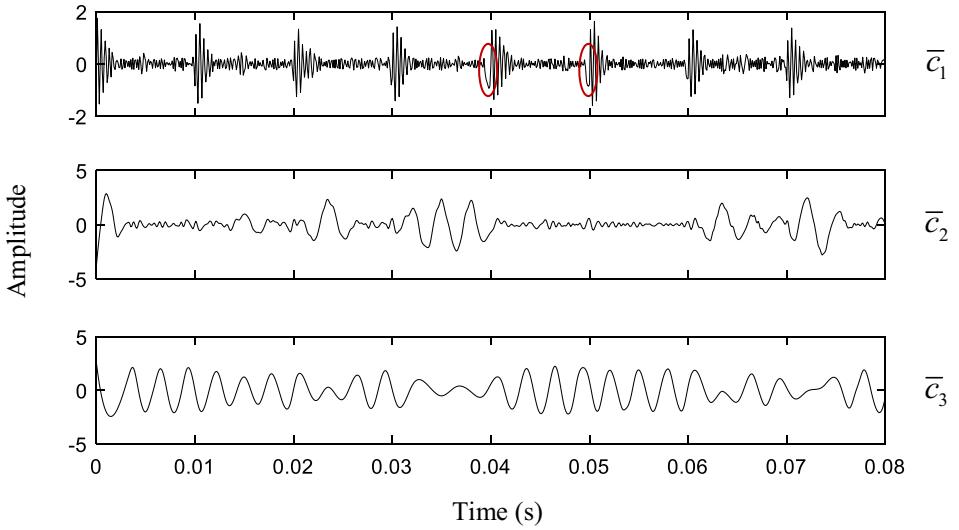

Fig. 3. The first three IMFs of the simulated signal using the EEMD with $Ne = 100$ and $\beta = 0.01$.

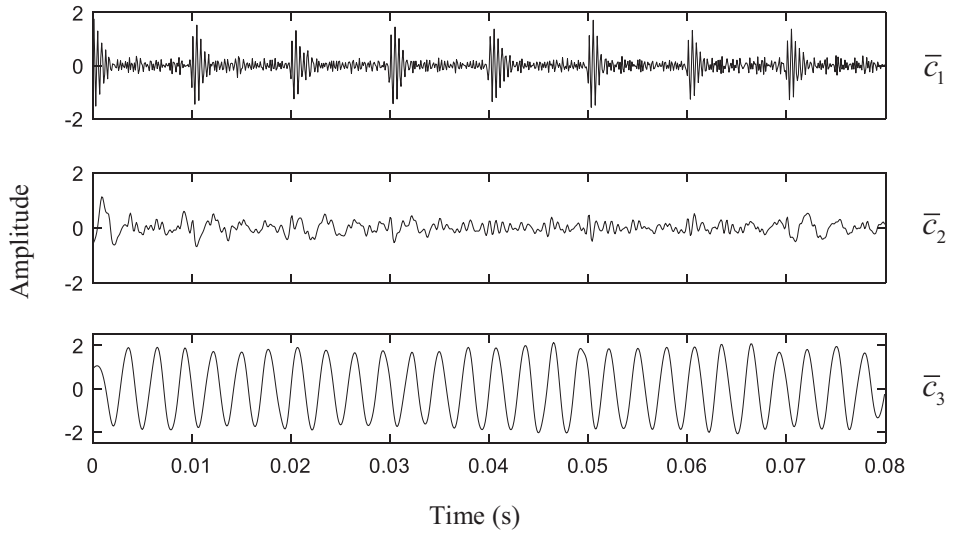

Fig. 4. The first three IMFs of the simulated signal using the EEMD with $Ne = 100$ and $\beta = 0.2$.

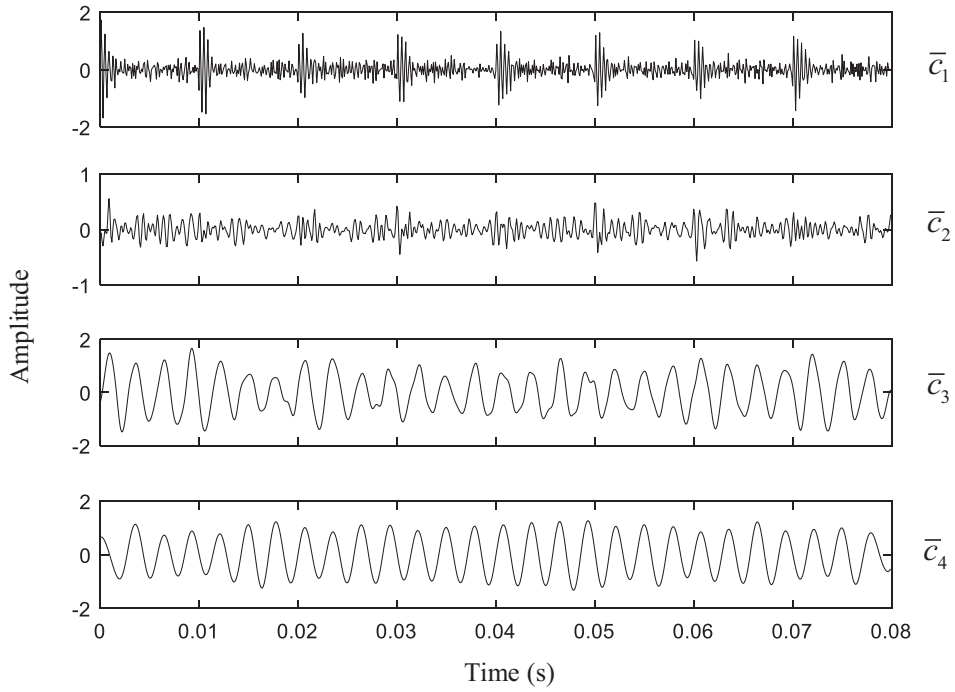

Fig. 5. The first four IMFs of the simulated signal using the EEMD with $Ne = 100$ and $\beta = 1$.

3. EMD manifold

Aiming to extract the true fault-related transients of rotating machines via the noise-assistance principle of the EEMD without an optimization of the noise amplitude, this paper proposes a new noise-assisted method, called EMD manifold (EMDM), which adaptively fuses the IMFs that are closely related to the fault, namely the sensitive modes, by a manifold learning algorithm. The sensitive modes are obtained through a small number of EMD trials on the signals plus white noise of different amplitudes, and constitute a high-dimensional data called sensitive mode matrix (SMM). In the SMM, the fault-related transients are embedded in each dimensional data, thus can be viewed as the intrinsic impulsive structure of the SMM that corresponds to a kind of nonlinear manifold. The oscillatory modes at different dimensions of the SMM are slightly variable, which is caused by the possible mode mixing phenomenon and the different amounts of residual noise. The sen-

sitive modes at different dimensions can be regarded as different samples of the underlying manifold. By addressing a manifold learning algorithm on the SMM, the true fault-related transients are supposed to be extracted, while other components and the noise (self-contained or added) contained in the SMM are removed.

For a vibration signal $x(t)$ with a localized machine fault, the EMDM algorithm for manifold learning of true fault-related transients mainly includes three procedures: sensitive mode locating, SMM construction and EMDM feature learning. To improve the adaptivity of the SMM to different signals, the second and last procedures are iterated until a certain condition is satisfied, as illustrated in Fig. 6. The following subsection will depict the details of the proposed algorithms.

3.1. Sensitive mode locating

The fault information mainly exists in the sensitive modes among the IMFs of $x(t)$ obtained by the EMD. Thus, the sensitive modes should be automatically located for further study. Moreover, the computational efficiency of the proposed method can be improved if the positions of the sensitive modes are firstly detected, because the decomposition of each EMD trial can be immediately stopped once the sensitive modes are obtained. Due to the possible mode mixing phenomenon of the EMD and/or the possible phenomenon of multiple resonance modulations in the vibration signal, there may be more than one sensitive modes in the decomposition results of each EMD trial. This paper focuses on the sensitive mode obtained in each EMD trial that contains the most fault information. Therefore, the EMD is first conducted on the original signal $x(t)$ to locate the most representative sensitive mode.

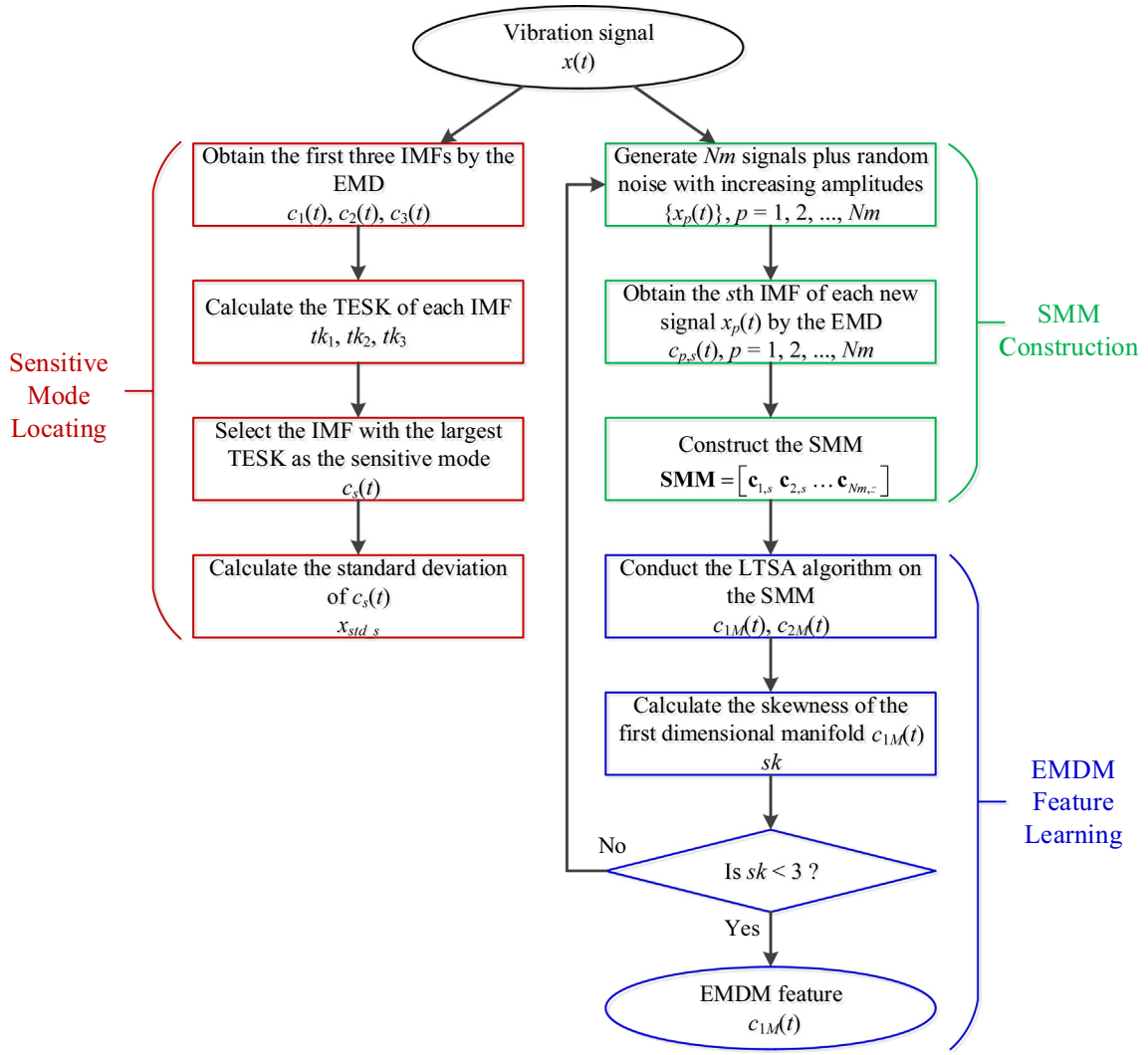

Fig. 6. Flowchart of proposed EMDM method for fault diagnosis of rotating machines.

Some techniques have been proposed to select the sensitive modes. He et al. [12] proposed a variance regression approach to select the most sensitive mode. Yan and Gao [33] proposed two criteria, the energy measure and correlation measure to determine the most sensitive mode. Lei and Zuo [34] selected the sensitive modes by measuring both the correlation between the vibration signal to be studied and its IMFs, and the correlation between the IMFs and a vibration signal collected from normal rotating machinery. Wang et al. [35] selected the IMF with the biggest kurtosis index value as the most sensitive mode. In the work of [36], three indexes, kurtosis, energy and approximate entropy, are combined for the selection of sensitive modes. Nevertheless, all the criteria mentioned above are derived from the time-domain waveforms of the obtained IMFs, which ignores the frequency-domain characteristics of the sensitive modes.

It is well known that kurtosis is a good measure to characterize the fault-related repetitive transients in the time domain, but is affected by outliers such as a random noise impulse [37]. The envelope spectrum of a sensitive mode contains the peaks of fault characteristic frequency and its harmonics and, therefore, can also be characterized by the kurtosis [38]. The kurtosis of signal envelope spectrum may also be affected by the outliers. Therefore, this paper combines the kurtosis in the time domain and the envelope spectrum domain to alleviate the effect of the outliers for the selection of the most representative sensitive mode. The new criterion is called time and envelope spectrum kurtosis (TESK), and is formulated by:

$$tk = k_c \cdot k_{es} \tag{7}$$

where

$$k_c = \frac{E(c(t) - \mu_c)^4}{\sigma_c^4} \tag{8}$$

$$k_{es} = \frac{E(es(f) - \mu_{es})^4}{\sigma_{es}^4} \tag{9}$$

with $c(t)$ as the IMF to be analyzed, μ_c as the mean of $c(t)$, σ_c as the standard deviation of $c(t)$, $E(\cdot)$ as the expectation operator, $es(f)$ as the power spectrum of the envelope of $c(t)$, μ_{es} as the mean of $es(f)$, σ_{es} as the standard deviation of $es(f)$.

In the EMD representation of a signal, the fast oscillation components are contained in the lower-order IMFs, while the slow oscillations are contained in the higher-order IMFs. Due to that the fault-related transients belong to the fast oscillations, only the first three IMFs of the original signal $x(t)$ are obtained in the procedure of sensitive mode locating. The TESKs of the three IMFs are calculated, and the IMF with the largest TESK is selected as the sensitive mode, whose location is denoted by s ($\in \{1, 2, 3\}$). Hence, the sensitive mode derived from the original signal is denoted by $c_s(t)$.

3.2. SMM construction

In order to reveal the underlying manifold structure of the fault-related transients via the manifold learning method, a high-dimensional data in which the manifold of transients is embedded should be first constructed. The sensitive mode $c_s(t)$ is obtained by conducting the EMD on the original signal, which is just one sample of the underlying manifold. The adding of random noise to the original signal can produce different samples via the EMD method. Therefore, this paper conducts Nm EMD trials on the signals plus white noise of different amplitudes to construct the high-dimensional data, i.e., the Nm-dimensional SMM. First, Nm signals plus noise are generated by

$$x_p(t) = x(t) + \beta_p x_{std\_s} n_p(t), \ p = 1, 2, \ldots, Nm \tag{10}$$

where $n_p(t)$ is a zero-mean unit-variance white noise for the pth trial, x_{std_s} is the standard deviation of the sensitive mode $c_s(t)$, β_p is the ratio of the standard deviation of the noise to x_{std_s}, and $\beta_p \in [0.01, \ 1]$. x_{std_s} rather than x_{std} in Eq. (5) is used in the proposed method because only the sensitive mode is the interest of this paper. Then, each noise-added signal $x_p(t)$ (p = 1, 2, …, Nm) is separately decomposed using the EMD until the sth IMF $c_{p,s}(t)$ is obtained, where $c_{p,s}(t)$ is the sensitive mode of the pth EMD trial. Finally, the SMM is constructed by the Nm sensitive modes as

$$\mathbf{SMM} = [\mathbf{c}_{1,s} \ \mathbf{c}_{2,s} \ \ldots \ \mathbf{c}_{Nm,s}] \tag{11}$$

where $\mathbf{SMM} \in \mathbf{R}^{N \times Nm}$, and $\mathbf{c}_{p,s} (\in \mathbf{R}^{N \times 1})$ is $c_{p,s}(t)$ in the discrete format with the length of N.

In the SMM, the sensitive modes with small added noise amplitudes would contain relatively small residual noise, while those with large amplitudes would not be corrupted by the residual components resulted from the mode mixing problem. Therefore, every dimensional data in the SMM is helpful for the learning of the manifold feature of the fault-related transients, i.e., the EMDM, which will be achieved in the following subsection.

3.3. EMDM feature learning

There have been proposed several manifold learning algorithms during the past a few years. The local tangent space alignment (LTSA) algorithm [39] is employed for the EMDM feature learning in this paper, because it has been proved to be robust and effective for the extraction of impulsive feature [31,32]. The SMM constructed in Eq. (11) can be rewritten as

$$\mathbf{SMM} = \begin{bmatrix} \mathbf{y}_1 \\ \mathbf{y}_2 \\ \cdots \\ \mathbf{y}_N \end{bmatrix} \tag{12}$$

where $\mathbf{y}_i (\in \mathbf{R}^{1\times Nm})$ is the ith point in the Nm-D data space. In the LTSA algorithm, the data points $\mathbf{y}_i$ ($i = 1, 2, \ldots, N$) are assumed to lie on or near a nonlinear manifold with intrinsic dimension Nd ($<Nm$). And the nonlinear manifold is assumed to be locally linear. Thus, there exists a linear mapping from a high-dimensional space to its local tangent space, and also a linear mapping from the corresponding low-dimensional manifold to the same local tangent space. The local projections of the neighbors on the tangent space at each data point $\mathbf{y}_i$ in the SMM would be kept in the low-dimensional manifold after aligning them in the global coordinates. To reach this goal, q-nearest neighbors of each $\mathbf{y}_i$ is selected to extract the local information on the tangent space of $\mathbf{y}_i$, which are used to construct an alignment matrix $\mathbf{B}$. There exists an affine error from the local tangent space coordinates to the low-dimensional global representation. The affine error is minimized by calculating the eigenvectors $\mathbf{C}_M$ of $\mathbf{B}$ as

$$\mathbf{C}_M = [\mathbf{c}_{1M}\ \mathbf{c}_{2M}\ \ldots\ \mathbf{c}_{NdM}] \tag{13}$$

with the column vectors $\mathbf{c}_{iM}$ ($i = 1, 2, \ldots, Nd$) corresponding to the Nd smallest nonzero eigenvalues of $\mathbf{B}$. For details and derivations of the LTSA algorithm, please refer to [39].

The eigenvectors $\mathbf{C}_M (\in \mathbf{R}^{N\times Nd})$ are the Nd-D global coordinates of the local tangent space, and are regarded as the low-dimensional manifold embedded in the high-dimensional **SMM**. $\mathbf{c}_{iM} \in \mathbf{R}^{N\times 1}$ is the ith dimensional data of $\mathbf{C}_M$ with the length of N, whose continuous format is $c_{iM}(t)$. Due to that the first dimensional data $c_{1M}(t)$ corresponds to the smallest nonzero eigenvalue of $\mathbf{B}$, and has the minimum reconstruction error, it can well reflect the intrinsic manifold structure related to the fault-related transients. Thus, $c_{1M}(t)$ is taken as the EMDM feature in this paper.

In the LTSA algorithm, there are two parameters, viz. the number of nearest neighbors q and the intrinsic dimension Nd, that should be determined. In this paper, q is set as $Nm + 3$ according to [40], Nd is set as 2 in order that some residual information survived in the manifold output is divided into the second dimensional data $c_{2M}(t)$.

The idea of the LTSA is based on the keep of local liner approximation of the data neighborhoods from high-dimensional data to low-dimensional manifold. However, there are cases when the local liner approximation is not accurate, leading to a bad performance of the LTSA. As for the EMDM feature learning in this paper, the fault-related transient impulses may not have equal absolute amplitudes between the upper and lower waveforms, i.e., the obtained waveform is not symmetrical in the up-and-down direction, which is not the true signal structure when a localized fault occurs. One way to improve the performance is to change the number of nearest neighbors q for a better local liner approximation [31]. This paper adopts another way to achieve a satisfactory EMDM feature, that is to adjust the local data distribution with the assistance of random noise. In the previous subsection, the SMM is constructed by selecting the sensitive modes after performing the EMD on the multiple noise-added signals. The noise added are random. Thus the sensitive modes at the same dimension of the SMM are slightly different when repeating the SMM construction, which would affect the local data distribution of the SMM. The symmetry of the EMDM feature can be evaluated by the skewness criterion, as formulated below:

$$sk = \frac{E(c_{1M}(t) - \mu_M)^3}{\sigma_M^3} \tag{14}$$

where μ_M is the mean of $c_{1M}(t)$, σ_M is the standard deviation of $c_{1M}(t)$. As can be seen in Fig. 6, the iteration of the feature learning will stop if sk is smaller than 3, at which time the symmetry of $c_{1M}(t)$ is satisfactory.

3.4. Summary of the proposed method

In summary, the proposed EMDM algorithm is presented in Fig. 6 and described as follows:

1) Obtain the first three IMFs $c_1(t)$, $c_2(t)$ and $c_3(t)$ by conducting the EMD on the original vibration signal $x(t)$.
2) Calculate the TESK of each IMF via Eq. (7). Then, three TESK values tk_1, tk_2 and tk_3 are obtained.
3) Select the IMF with the largest TESK as the sensitive mode of $x(t)$, which is denoted by $c_s(t)$ and $s \in \{1, 2, 3\}$.
4) Calculate the standard deviation x_{std_s} of $c_s(t)$.
5) Generate Nm signals plus random noise with increasing amplitudes via Eq. (10). A signal series $\{x_p(t)\}$ ($p = 1, 2, \ldots, Nm$) is then obtained.
6) Obtain the sth IMF of each new signal $x_p(t)$ by the EMD, which is denoted by $c_{p,s}(t)$ and is viewed as the sensitive mode of $x_p(t)$.
7) Construct the SMM by the obtained Nm sensitive modes via Eq. (11).
8) Conduct the LTSA algorithm on the SMM with $Nd = 2$ and $q = Nm + 3$. A 2-dimensional manifold $\mathbf{C}_M$ is obtained with each dimensional signal denoted by $c_{iM}(t)$ ($i \in \{1, 2\}$).
9) Calculate the skewness sk of the first dimensional manifold $c_{1M}(t)$ via Eq. (14).
10) Is sk smaller than 3?

a) No. Repeat steps 5)–10).
b) Yes. Save $c_{1M}(t)$ as the EMDM feature for fault identification.

Since the LTSA is a nonlinear method, the proposed EMDM is the fusion of the sensitive modes in a nonlinear way, which is supposed to be better than the linear average by the EEMD and its variations on mode mixing alleviation and noise removal. Due to the excellent feature extraction capability of the LTSA, the solid fault-related transients will be reserved for their inherent manifold form, while the unrelated components and noise will be abandoned as they are random information among the high-dimensional data. Therefore, the achieved EMDM feature can reveal the factual impulsive structure of the fault-related transients. Moreover, the proposed method is adaptive to different signals of rotating machines because different amplitudes of the added noise are considered and the local liner approximation in the EMDM learning is optimized.

3.5. Demonstration of the proposed method

The simulated signal shown in Fig. 1(d) is analyzed by the proposed method to demonstrate its effectiveness. First, the signal is decomposed by the EMD method to locate the sensitive mode. The kurtosis in the time domain k_c defined by Eq. (8), the kurtosis in the envelope spectrum domain k_{es} defined by Eq. (9), and their combination criterion TESK tk defined by Eq. (7) of the first three IMFs (shown in Fig. 2) are calculated, and the values are plotted in Fig. 7. It is clear that the first IMF $c_1(t)$ is the sensitive mode, as can be seen in Fig. 2. By comparing the values of different criteria shown in Fig. 7, the sensitive mode is correctly located at the first position by the k_c criterion, while is located wrong at the second position by the k_{es} criterion, and is correctly located by the combined tk criterion. Therefore, the proposed TESK criterion can avoid the effect of outliers on the envelope spectra of the IMFs in this case.

Then, ten new signals with added noise of increasing amplitudes are generated via Eq. (10) and are decomposed by the EMD. The decompositions are all stopped when the first IMFs (i.e., the sensitive modes) are obtained. The SMM is formed by the ten sensitive modes obtained, which are also displayed in Fig. 8. It can be seen that, with the increase of added noise amplitude, the mode mixing phenomenon occurred in the sensitive mode disappears, while the noise level survived in the sensitive mode increases. It is difficult to determine which one is the best among the sensitive modes with different added noise amplitudes. Without considering the selection of the best sensitive mode, the ten sensitive modes are all used for EMDM feature learning. The feature learning process iterates until the sk of the first dimensional manifold is less than 3, as shown in Fig. 9(a). Fig. 9(b) displays the first dimensional manifolds obtained in the last two iterations, whose sk values are 6.13 and 1.73, respectively. Due to that the fault-related transients are embedded in each sensitive mode with solid structures, while the unrelated components and noise are variable among different sensitive modes, the learned EMDM feature by the LTSA algorithm only reserve the former information, as illustrated in the bottom of Fig. 9(b), which reveals the factual impulsive structure of the fault-related transients, and is superior to all the sensitive modes shown in Fig. 8. In the top of Fig. 9(b), the transient impulses have larger negative amplitudes than positive amplitudes, leading to a larger skewness values as compared to the bottom waveform of Fig. 9(b). Therefore, the skewness criterion is suitable to evaluate the symmetry of the EMDM feature learning.

The proposed TESK criterion that is used for sensitive mode locating in subsection 3.1 is also used to compare the performance of different methods. The tk values of the original simulated signal, the results obtained by the EMD, the EEMD with $Ne = 100$ and $\beta = 0.2$, and the proposed EMDM are presented in Fig. 10. It can be seen that the EMDM

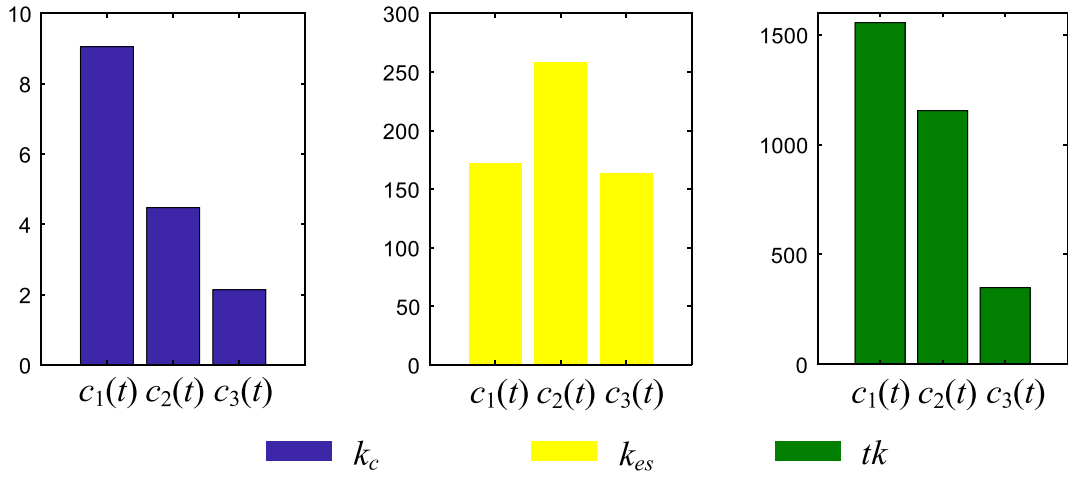

Fig. 7. Values of different criteria for sensitive mode locating of the simulated signal.

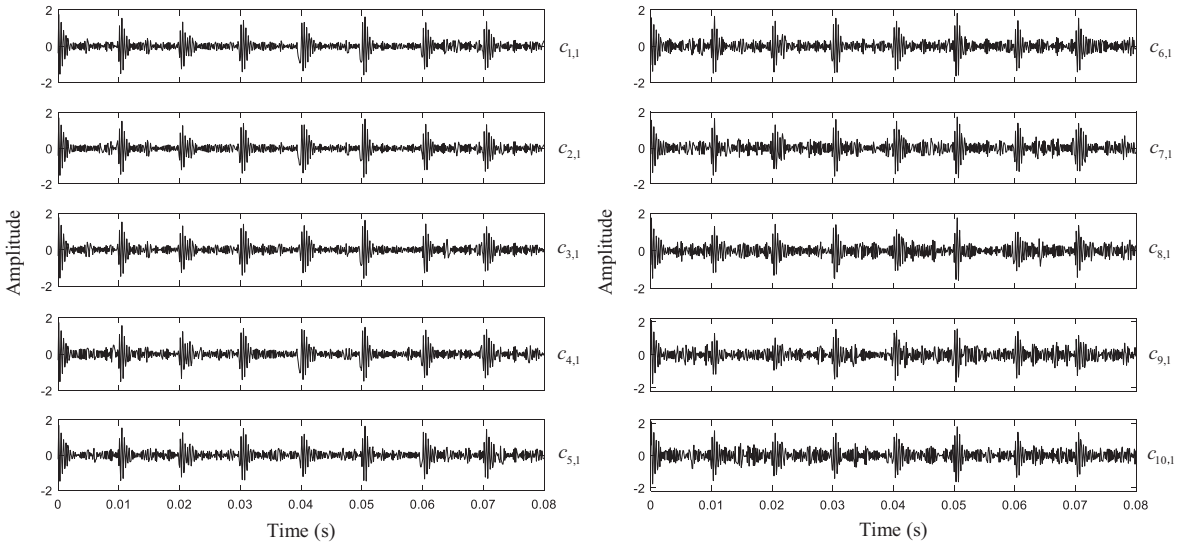

Fig. 8. Ten sensitive modes for SMM construction of the simulated signal.

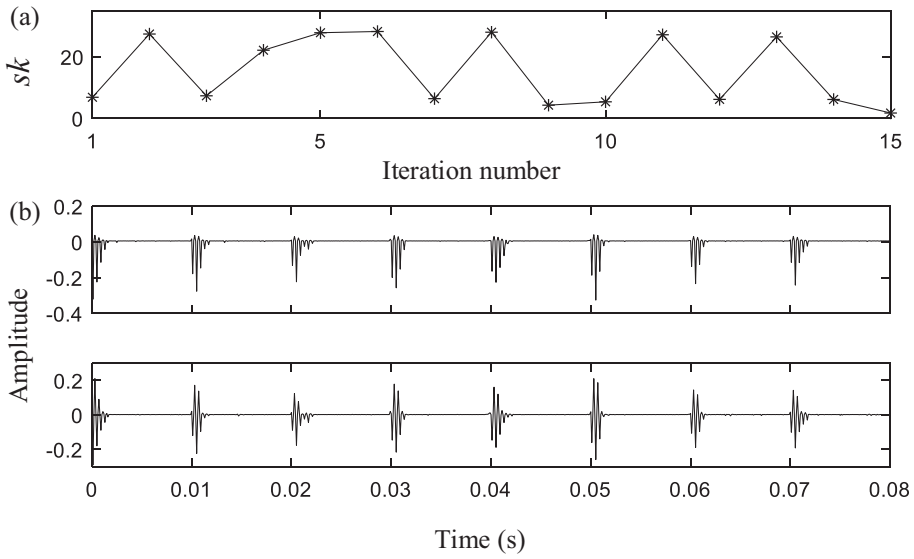

Fig. 9. Results of EMDM feature learning: (a) *sk* of the first dimensional manifold in each iteration; (b) the first dimensional manifolds obtained in the last two iterations.

method can achieve a great larger *tk* value than the EMD and EEMD methods, indicating its superiority over the traditional methods.

To investigate the effect of the SMM dimension *Nm* on the performance of the proposed EMDM, a series of simulations are carried out with different values of *Nm*. Due to the randomicity of the noise added in the EMDM method, the total iteration numbers and the learned EMDM feature would be different for the same parameters. Therefore, for each value of *Nm*, the simulated signal is processed via the EMDM method for ten times, and the mean values of the total iterations and the *tk* of the learned EMDM feature are calculated. The mean total iterations and mean *tk* values with the *Nm* ranging from 3 to 20 are presented in Fig. 11. It can be seen that the two curves both rise with the increase of *Nm* in the initial stage, then tend to be steady with small fluctuations after *Nm* reaches about 10. Because a larger *Nm* leads to a heavier computational burden in the proposed EMDM, *Nm* is set as 10 in this paper.

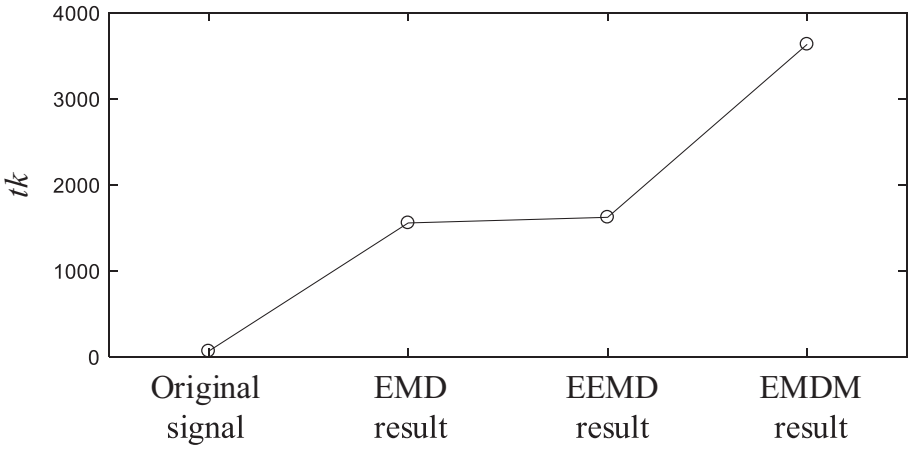

Fig. 10. *tk* values of the original signal and the results obtained by different methods for the simulated signal.

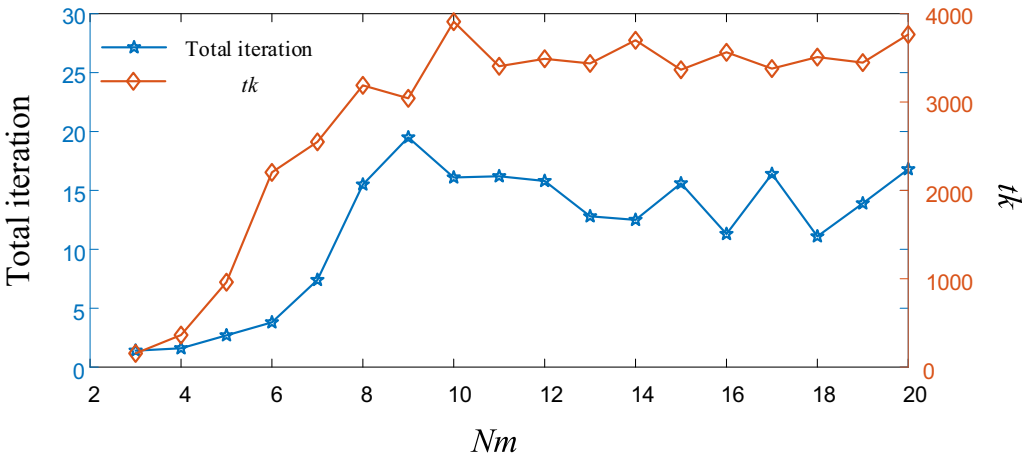

Fig. 11. Mean total iterations and *tk* values with different SMM dimension *Nm*.

4. Experimental verification

To validate the enhanced performance of the proposed EMDM method in practical applications to fault diagnosis of rotating machines, the experimental data from a gearbox run-to-failure test, a test rig with a seeded bearing fault, and a bearing run-to-failure test are analyzed successively.

4.1. Gearbox run-to-failure data

The run-to-failure test was carried out on an automobile transmission gearbox, which has 5 forward speeds and one backward speed, as shown in Fig. 12. The gearbox was loaded on the third speed, and the rotating speed of the input shaft was 1600 rpm in the experiment. According to the kinematic scheme of the gearbox, the meshing frequency of the gearbox is 500 Hz, and the rotating frequencies of the tested driving and driven gears are 20 Hz and 18.5 Hz, respectively. An accelerometer was mounted on the outer case of the gearbox for collection of vibration signals with a sampling frequency of 3 kHz. The data were recorded by the cycle, where one cycle means 700 thousand meshing times of the tested gears. One tooth of the tested driving gear broke at the beginning of the seventh cycle. The vibration signal at the sixth cycle is taken for analysis in this paper, at which time the tested driving gear had a wearing fault. The characteristic frequency of the defective gear is f_d = 20 Hz.

Fig. 13 shows the analyzed gearbox vibration signal with a gear wearing fault. It can be seen that the noise contained in the vibration signal is so heavy that the fault-induced impulses are hard to be identified. The EMD method is firstly used to analyze this signal. To locate the sensitive mode, the criteria of k_c, k_{es}, and *tk* are calculated for the first three IMFs, as presented in Fig. 14. The first IMF $c_1(t)$ is deemed the sensitive mode according to k_c, while the second IMF $c_2(t)$ is considered as

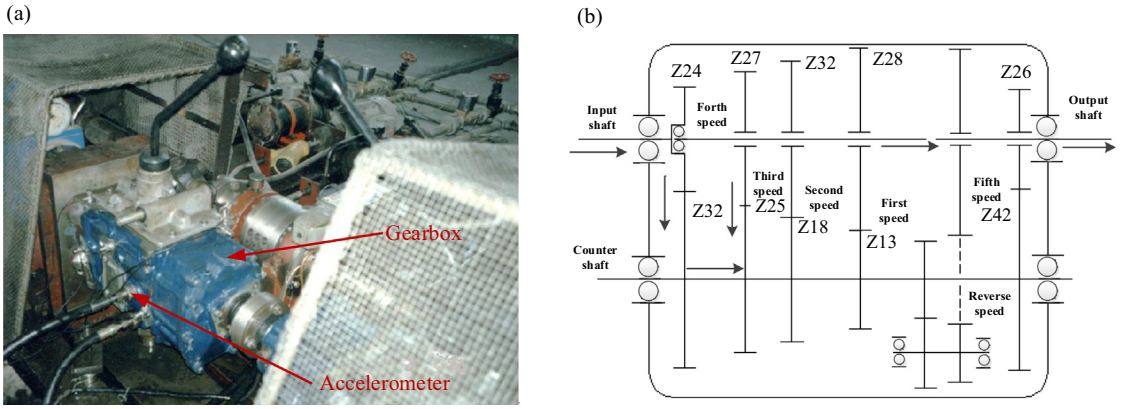

Fig. 12. Gearbox for run-to-failure test: (a) hardware setup; (b) kinematic scheme.

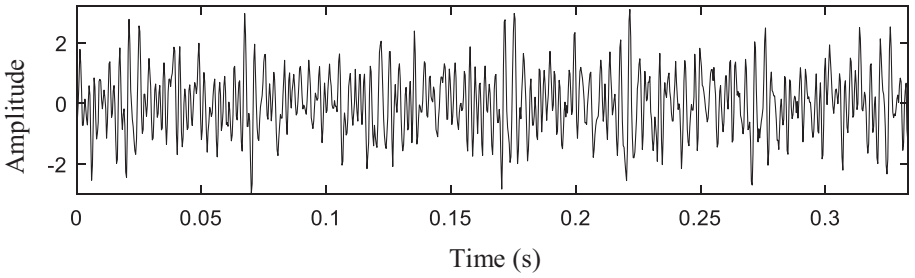

Fig. 13. Waveform of the gearbox vibration signal with a gear wearing fault.

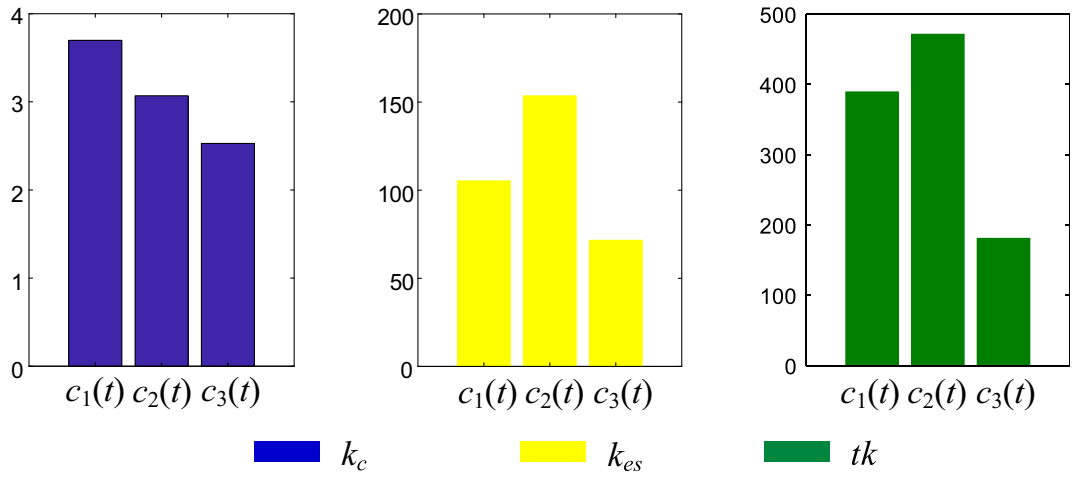

Fig. 14. Values of different criteria for sensitive mode locating of the gearbox vibration signal.

the sensitive mode according to k_{es}. By combining k_c and k_{es}, $c_2(t)$ is selected as the sensitive mode according to tk, which is shown in Fig. 15(a). The fault characteristic frequency f_d is identified in the envelope spectrum of $c_2(t)$, proving that the determination of the sensitive mode by tk is correct. However, the waveform of $c_2(t)$ still contains heavy noise; some fault-induced impulses cannot be discriminated from the noise.

The signal in Fig. 13 is then analyzed by the EEMD method with $Ne = 200$ and $\beta = 0.2$. Fig. 15(b) displays the second mode and its envelope spectrum. The noise in the envelope spectrum is lower than that in Fig. 15(a). The repetitive impulses can be identified in the waveform. However, the noise between the impulses has noticeable amplitudes.

The improved CEEMDAN method [29] is also introduced to analyze the gearbox vibration signal. This method has the ability to reduce the residual noise contained in the obtained IMFs. Fig. 15(c) shows the obtained sensitive mode and its envel-

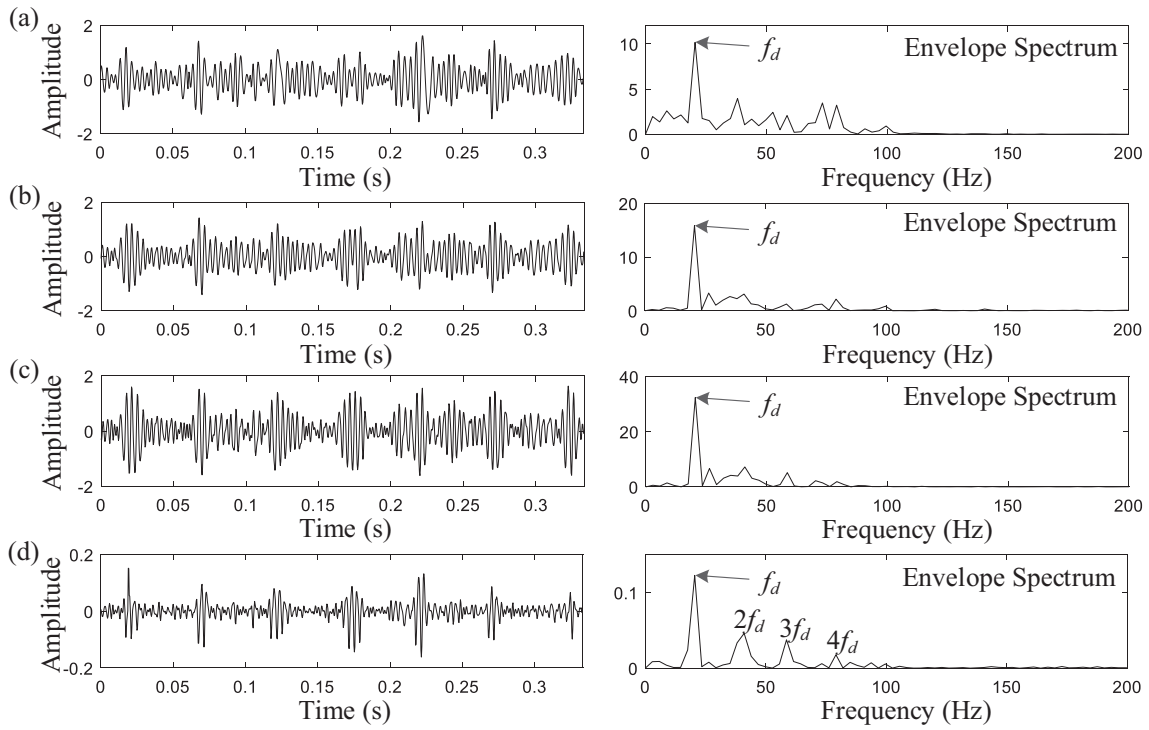

Fig. 15. Analyzed results of the gearbox vibration signal by different methods: (a) the EMD method; (b) the EEMD method; (c) the improved CEEMDAN method; (d) the proposed EMDM method.

ope spectrum with $Ne = 200$ and $\beta = 0.2$. The result indicates only slight improvement in removal of noise from the sensitive mode as compared to the result shown in Fig. 15(b) by the EEMD method.

The proposed EMDM method is finally employed to analyze the signal in Fig. 13. The EMD method is successively performed on the signal with ten different noise added. The second IMFs shown in Fig. 16 of all the decompositions are selected to construct the SMM for EMDM feature learning. As can be seen in Fig. 16, the noise level contained in the sensitive modes increases from $c_{1,2}(t)$ to $c_{10,2}(t)$. Some fault-induced impulses are corrupted by the noise in some sensitive modes, while are enhanced by the noise in other sensitive modes. Fig. 17 displays the envelope spectra of the ten sensitive modes in Fig. 16.

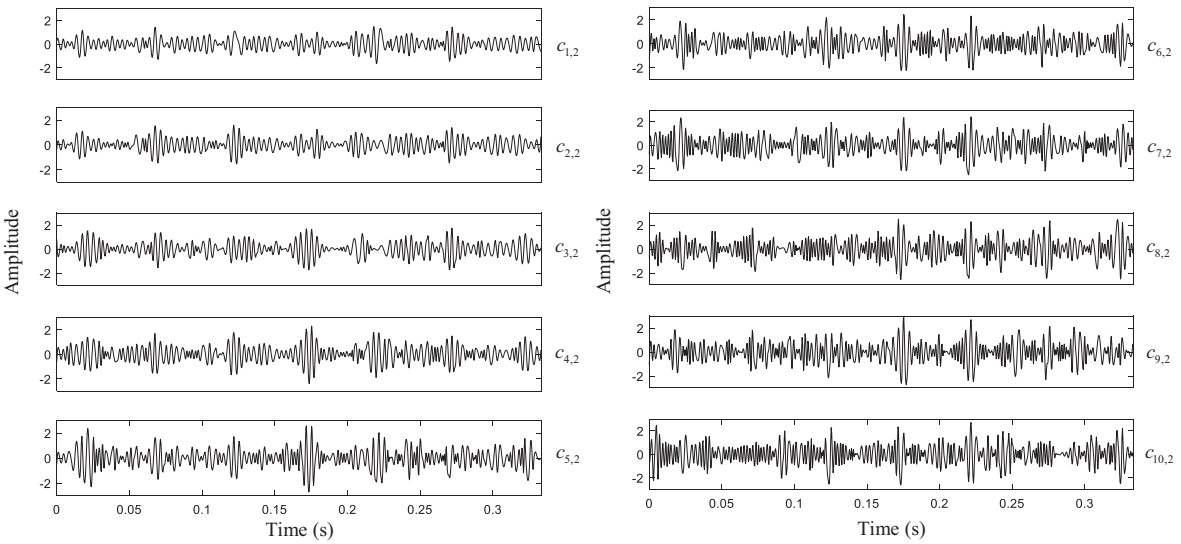

Fig. 16. Ten sensitive modes for SMM construction of the gearbox vibration signal.

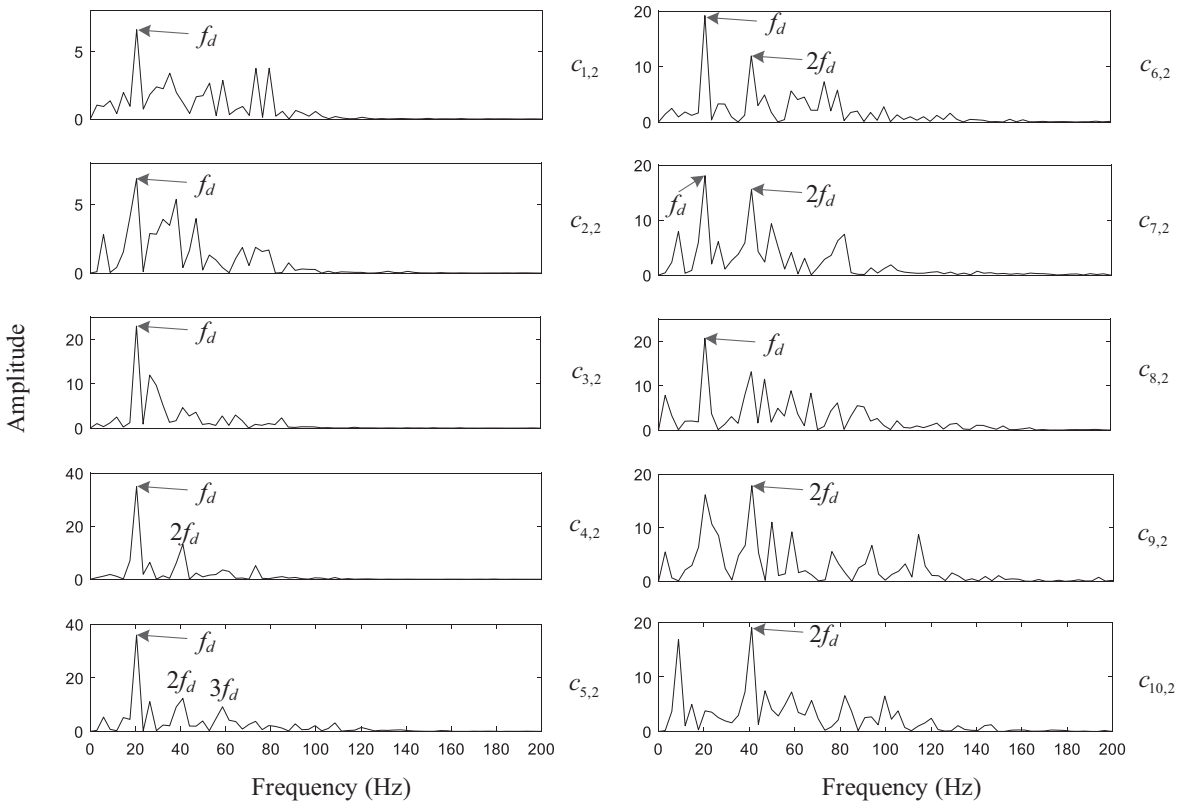

Fig. 17. Envelope spectra of the ten sensitive modes in Fig. 16.

Different envelope spectrum contains different noise interfering frequencies. Some envelope spectra are dominated by the fault characteristic frequency f_d, while others contain the second harmonic of f_d. Therefore, each sensitive mode is helpful for the EMDM feature learning. The feature learning process repeats 14 times until the *sk* of the first dimensional manifold descends to be 0.57 from above 3. The learned EMDM feature is provided in Fig. 15(d), along with the corresponding envelope spectrum. In the waveform, the fault-induced impulses are extracted, and the noise between them are much suppressed as compared to those in Figs. 15(a)–(c) and 16, leading to a more distinct presentation for identification of fault-related transients. In the envelope spectrum, the second to fourth harmonics of the fault characteristic frequency are excited, and the noise interfering frequencies are removed, which facilitates the fault detection.

To quantitatively compare the performance of the four methods, the *tk* values of the original signal and the analyzed results given in Fig. 15 are computed and presented in Fig. 18. It can be seen that, each *tk* value is larger than the last, which demonstrates that the performance is improved one by one via the EEMD, the improved CEEMDAN, and the EMDM methods. Furthermore, the proposed EMDM method achieves a large advancement over the existing methods according to the rising range of the *tk* values. This experiment proves that the proposed EMDM method is superior to the EMD method and its variations in gearbox fault diagnosis.

4.2. Data of bearing with a seeded fault

To verify the effectiveness of the proposed method in bearing fault detection, a simplified bearing test stand was established, as shown in Fig. 19. The test stand consists of an induction driving motor, a shaft coupling to the motor and supported by two bearings, and a spring-loaded device as radial loader of the shaft. The supporting bearing installed at the right end of the shaft is the tested bearing, whose type is N306E. A single slit defect was seeded in the inner raceway of a new bearing by electro-discharge machining for signal acquisition of the seeded bearing fault. The width of the slit is 0.5 mm. A microphone with the type of INV9206 was put near the tested bearing for measurement of bearing acoustic signals with a sampling frequency of 20 kHz. The shaft run at the speed of 1464.6 rpm in a noisy environment in the experiment. The bearing characteristic frequency of the inner-race fault is calculated as $f_{\mathrm{BPFI}} = 146.5$ Hz.

Fig. 20 shows the waveforms of the bearing acoustic signals under healthy condition and seeded inner-race fault condition. The signal shown in Fig. 20(a) acquired when the bearing was healthy mainly contains the surrounding noise, and its amplitudes are commensurate with some fault-related transients in the signal shown in Fig. 20(b) acquired when the bear-

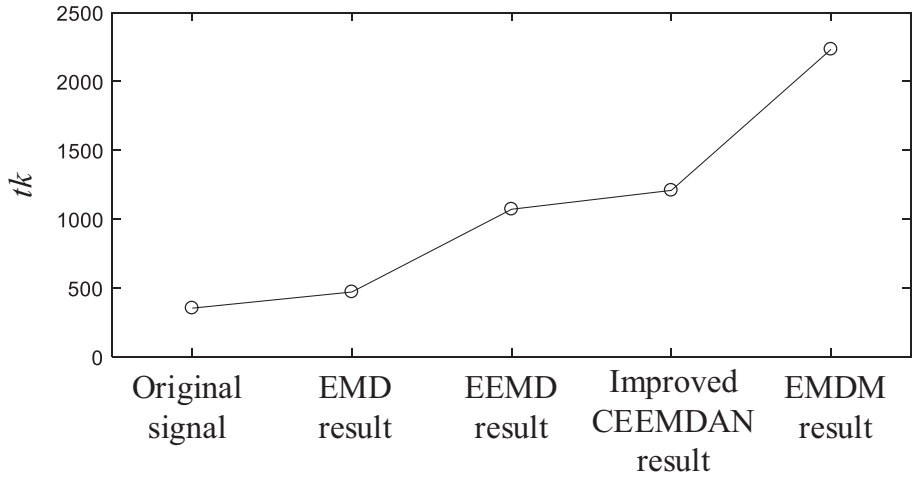

Fig. 18. *tk* values of the original signal and the results obtained by different methods for the gearbox vibration signal.

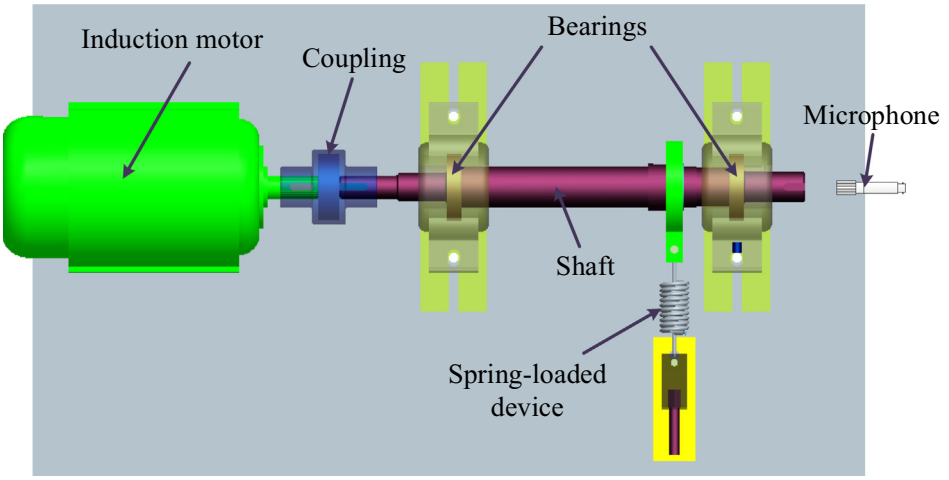

Fig. 19. Test stand of bearing with a seeded fault.

ing had the seeded inner-race fault. Therefore, some fault-related transients are not observable in the signal shown in Fig. 20 (b). The signal with the inner-race fault is analyzed by the EMD, the EEMD, the improved CEEMDAN, and the proposed EMDM methods, successively. The analyzed results are shown in Fig. 21. The noise retained in the first three results is obtrusive, while is totally removed in the last result. Moreover, the second harmonic of the bearing inner-race fault characteristic frequency in the envelope spectrum in Fig. 21(d) is relatively higher than those in Fig. 21(a)–(c). The *tk* values of the original signal shown in Fig. 20(b) and the results shown in Fig. 21 are displayed in Fig. 22. The EMDM method achieves a much higher *tk* value than the other methods. Therefore, the performance of the bearing inner-race fault detection is greatly enhanced by the proposed method.

4.3. Bearing run-to-failure data

To further confirm the enhanced performance of the proposed method in bearing fault detection, a bearing vibration signal with an incipient fault is analyzed in this subsection. The faulty bearing evolved from a healthy bearing in a bearing run-to-failure test made by the University of Cincinnati. The details of the experiment can be found in Ref. [41]. An outer-race failure occurred in the tested bearing at the end of the experiment. The bearing characteristic frequency of the outer-race fault is calculated to be $f_{BPFO} = 236.4$ Hz. A vibration signal in the early stage of the damage propagation [2] is shown in Fig. 23. There is no sign of the fault-related repetitive transients due to weak fault impacts and large vibration noise.

The EMD, the EEMD, the improved CEEMDAN, and the proposed EMDM methods are applied to analyze the bearing vibration signal. The analyzed results are displayed in Fig. 24. The fault-related impulses are exposed by all the methods. However,

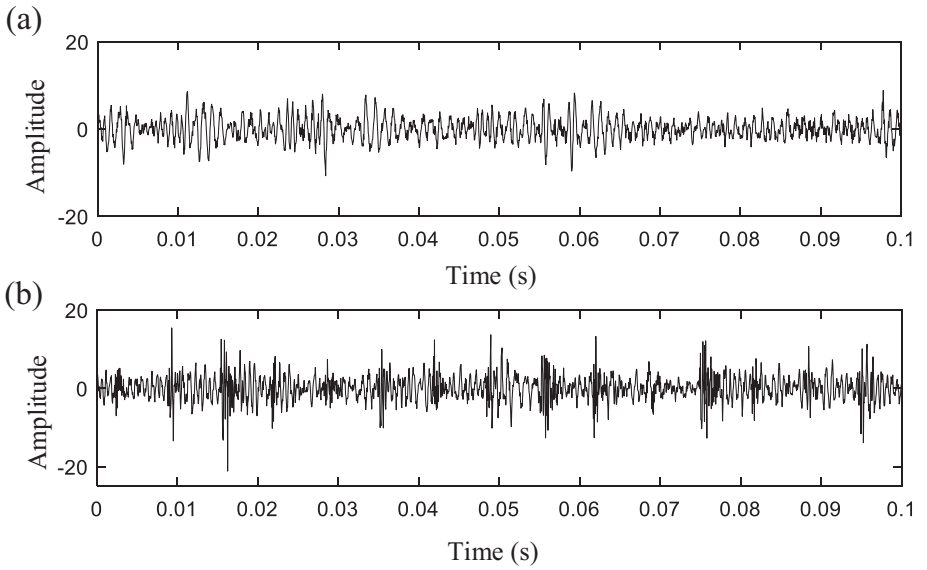

Fig. 20. Waveforms of the bearing acoustic signals under (a) healthy condition and (b) inner-race fault condition.

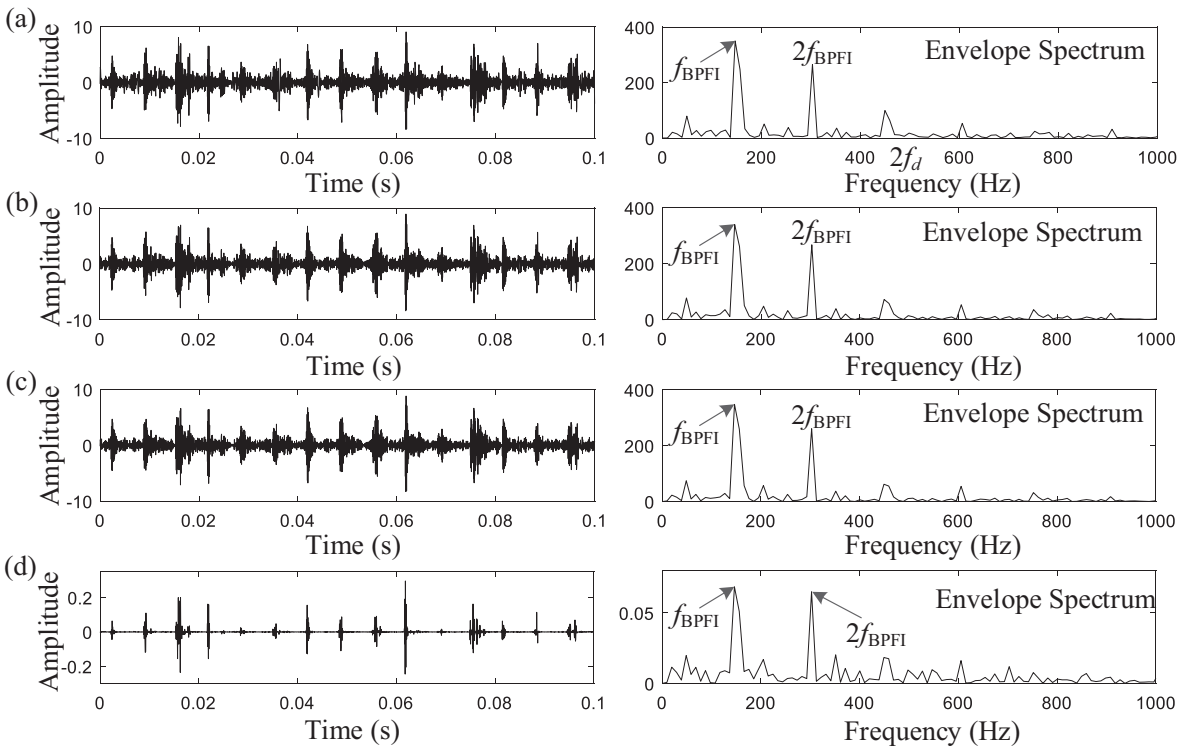

Fig. 21. Analyzed results of the bearing acoustic signal with an inner-race fault by different methods: (a) the EMD method; (b) the EEMD method; (c) the improved CEEMDAN method; (d) the proposed EMDM method.

the EEMD and the improvement CEEMDAN methods show little improvement in residual noise suppression over the EMD method. On the contrary, the noise contained in the waveform of Fig. 24(d) has small amplitude, resulting in a more distinguishing representation for fault identification. Furthermore, the third harmonic of the bearing outer-race fault characteristic frequency has too small amplitude to be distinguished from interfering frequencies in the envelope spectra of Fig. 24(a)–(c), while is raised evidently in the envelope spectrum of Fig. 24(d). As can be seen in Fig. 25, the *tk* values of the analyzed results

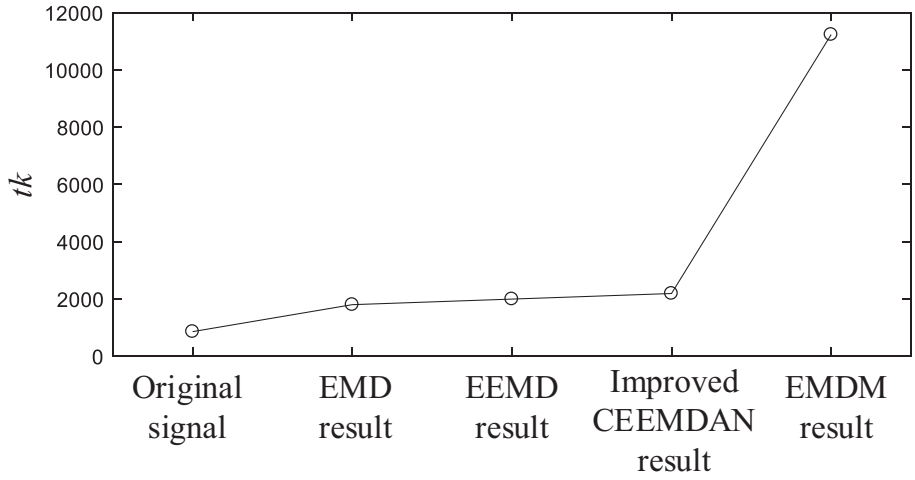

Fig. 22. *tk* values of the original signal and the results obtained by different methods for the bearing acoustic signal with an inner-race fault.

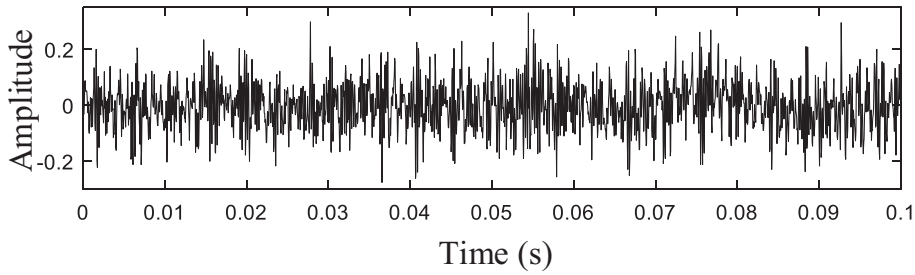

Fig. 23. Waveform of the bearing vibration signal with an incipient outer-race fault.

exhibit an absolute predominance of the proposed method over the other methods. This case verifies the enhanced performance of the proposed EMDM method in bearing fault detection again.

4.4. Discussion

To realize an enhanced identification of the fault-related transients of rotating machines, this paper has proposed a new noise-assisted EMDM method, by which the sensitive modes with different noise are fused nonlinearly and adaptively. The simulated and experimental cases above have proved that the proposed EMDM method can highlight the fault-related transients while suppress the fault-unrelated components and, therefore, can greatly improve the TESK criterion compared to the EEMD and its variations. The improvement mainly benefits from the random amplitude property of the white noise added and the powerful nonlinear feature extraction capability of the LTSA algorithm. With the aid of white noise added, different samples of the manifold structure of the fault-related transients are obtained, among which the fault-unrelated components vary, which is helpful for the true mode extraction of the fault-related transients by the manifold learning method. Furthermore, the accuracy of the proposed method is affected if the nonlinearity of the underlying manifold of the SMM is severe, because in this condition the local liner approximation of the SMM is not accurate in the LTSA algorithm, as is illustrated in the top waveform of Fig. 9(b). The repetitive adding of white noise is a way to adjust the local data distribution of the SMM constructed, by which a nonlinearity-reduced underlying manifold of the SMM constructed can be produced, leading to a satisfactory EMDM feature that is adaptive to different signals of rotating machines, as is proved by the bottom waveform of Fig. 9(b). Nevertheless, since the proposed method does not use the zero-mean property of the white noise to decrease the residual noise, the adding of other kinds of noise in the EMDM method will be explored in the future.

It should be noted that, the proposed method focuses on the extraction of the fault impulsive transients which are amplitude modulation components in the measured signals. For the faults that exhibit frequency modulation components in the measured signals, the sensitive mode locating method based on the proposed TESK criterion may not be effective, and the extraction of this kind of fault features by the manifold learning method remains to be investigated.

In the proposed EMDM method, the sensitive modes are located at a fixed position in different EMD trials. It is possible that the sensitive modes are located at different positions when repeating adding random noise [29], making it difficult to

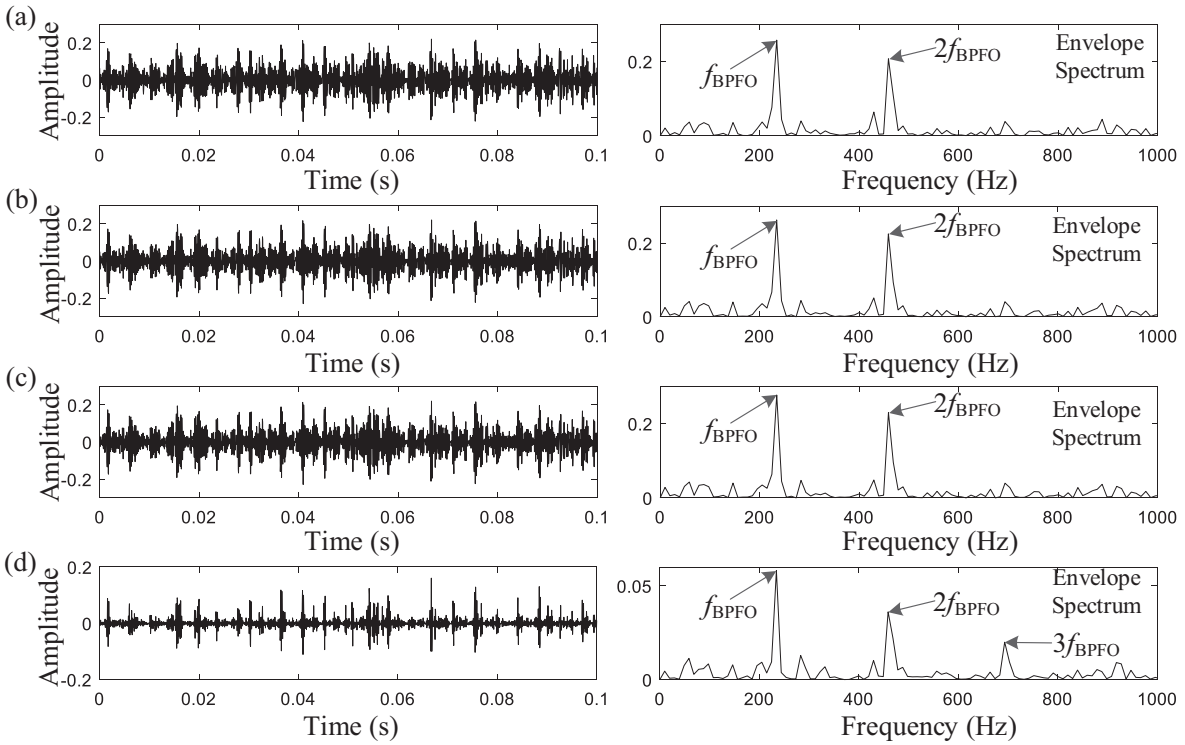

Fig. 24. Analyzed results of the bearing acoustic signal with an incipient outer-race fault by different methods: (a) the EMD method; (b) the EEMD method; (c) the improved CEEMDAN method; (d) the proposed EMDM method.

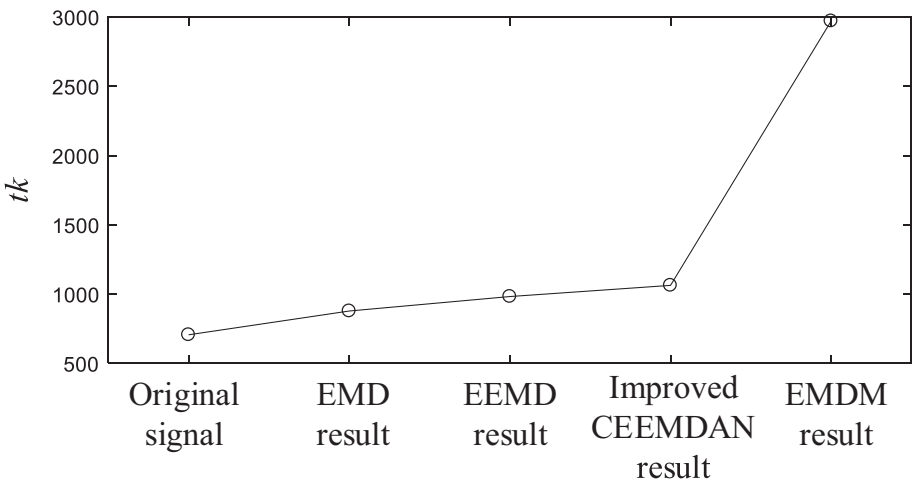

Fig. 25. *tk* values of the original signal and the results obtained by different methods for the bearing acoustic signal with an incipient outer-race fault.

construct the SMM for EMDM feature learning. In this condition, the sensitive mode in each EMD trial should be located separately according to the TESK criterion. The strategies of noise adding and decomposition in the improved CEEMDAN method [29] is also a way to tackle this problem, which will be studied in our future work.

5. Conclusions

This paper has proposed a new method, called EMDM, for enhanced fault diagnosis of rotating machines. The major contribution is that the sensitive modes containing the fault information and different noise are fused adaptively via a nonlinear manifold learning method. The fault-unrelated components in the sensitive modes, including the mode-mixing-induced

components and the residual noise derived from both added and self-contained noise, can be removed by the proposed method. Hence the learned EMDM feature can represent the true fault-related transients of rotating machines. New TESK criterion has been designed to locate the sensitive mode among the IMFs of the EMD method automatically, and has also been used for quantitative comparison of the performance of different methods. Local data distribution of the high-dimensional SMM was adjusted by random noise of different amplitudes added to guarantee satisfactory symmetry of the EMDM feature. Skewness criterion has been adopted to evaluate the symmetry of the EMDM feature. The proposed method has been successfully applied to analyze signals measured from a gearbox and two bearings with different faults. Its effectiveness and superiority over the EEMD and its variations have been confirmed by the experimental results, proving that the proposed EMDM method is promising for enhanced fault diagnosis of rotating machines.

Acknowledgments

This work was supported in part by the National Natural Science Foundation of China under Grants 51805342, 51875375 and 51875376, in part by the National Program for Support of Top-Notch Young Professionals, in part by the Natural Science Foundation of Jiangsu Province under Grant BK20180842, in part by the China Postdoctoral Science Foundation under Grant 2018M640514, and in part by the Jiangsu Planned Projects for Postdoctoral Research Funds under Grants 2018K006B and 2018K004C, in part by the Joint Fund of Equipment Pre-Research and Ministry of Education under grant 6141A02022141, in part by the Natural Science Fund for Colleges and Universities in Jiangsu Province under Grant 18KJB470022, and in part by the Suzhou Prospective Research Program under Grant SYG201912.

References

[1] R.B. Randall, J. Antoni, Rolling element bearing diagnostics-A tutorial, Mech. Syst. Signal Process. 25 (2011) 485–520.
[2] X. Jiang, J. Wang, J. Shi, C. Shen, W. Huang, Z. Zhu, A coarse-to-fine decomposing strategy of VMD for extraction of weak repetitive transients in fault diagnosis of rotating machines, Mech. Syst. Signal Process. 116 (2019) 668–692.
[3] L. Cui, X. Gong, J. Zhang, H. Wang, Double-dictionary matching pursuit for fault extent evaluation of rolling bearing based on the Lempel-Ziv complexity, J. Sound Vib. 385 (2016) 372–388.
[4] Q. He, E. Wu, Y. Pan, Multi-scale stochastic resonance spectrogram for fault diagnosis of rolling element bearings, J. Sound Vib. 420 (2018) 174–184.
[5] L. Song, H. Wang, P. Chen, Vibration-Based Intelligent Fault Diagnosis for Roller Bearings in Low-Speed Rotating Machinery, IEEE Trans. Instrum. Meas. 67 (2018) 1887–1899.
[6] C. Shen, Y. Qi, J. Wang, G. Cai, Z. Zhu, An automatic and robust features learning method for rotating machinery fault diagnosis based on contractive autoencoder, Eng. Appl. Artif. Intell. 76 (2018) 170–184.
[7] X. Ding, Q. He, N. Luo, A fusion feature and its improvement based on locality preserving projections for rolling element bearing fault classification, J. Sound Vib. 335 (2015) 367–383.
[8] D. Wang, K. Tsui, Brownian motion with adaptive drift for remaining useful life prediction: revisited, Mech. Syst. Signal Process. 99 (2018) 691–701.
[9] Y. Qian, R. Yan, R.X. Gao, A multi-time scale approach to remaining useful life prediction in rolling bearing, Mech. Syst. Signal Process. 83 (2017) 549–567.
[10] X. Li, Q. Ding, J.Q. Sun, Remaining useful life estimation in prognostics using deep convolution neural networks, Reliab. Eng. Syst. Saf. 172 (2018) 1–11.
[11] Y. Lei, J. Lin, Z. He, M.J. Zuo, A review on empirical mode decomposition in fault diagnosis of rotating machinery, Mech. Syst. Signal Process. 35 (2013) 108–126.
[12] Q. He, P. Li, F. Kong, Rolling bearing localized defect evaluation by multiscale signature via empirical mode decomposition, J. Vib. Acoust. 134 (2012) 061013.
[13] A. Rai, S.H. Upadhyay, Bearing performance degradation assessment based on a combination of empirical mode decomposition and k-medoids clustering, Mech. Syst. Signal Process. 93 (2017) 16–29.
[14] N.E. Huang, Z. Shen, S. Long, M. Wu, H. Shih, Q. Zheng, N.-C. Yen, C. Tung, H. Liu, The empirical mode decomposition and the Hilbert spectrum for nonlinear and non-stationary time series analysis, Proc. R. Soc. A Math. Phys. Eng. Sci. 454 (1998) 903–995.
[15] M. Zhao, J. Liu, Y. Wang, H. Zhu, On the EMD sifting property and instantaneous parameters, Adv. Data Sci. Adapt. Anal. 08 (2016) 1650010.
[16] K.J. Moore, M. Kurt, M. Eriten, D.M. McFarland, L.A. Bergman, A.F. Vakakis, Wavelet-bounded empirical mode decomposition for measured time series analysis, Mech. Syst. Signal Process. 99 (2018) 14–29.
[17] Z. Wu, N.E. Huang, Ensemble empirical mode decomposition: a noise-assisted data analysis method, Adv. Adapt. Data Anal. 01 (2009) 1–41.
[18] Y. Lei, N. Li, J. Lin, S. Wang, Fault diagnosis of rotating machinery based on an adaptive ensemble empirical mode decomposition, Sensors 13 (2013) 16950–16964.
[19] K. Yu, T.R. Lin, J.W. Tan, A bearing fault diagnosis technique based on singular values of EEMD spatial condition matrix and Gath-Geva clustering, Appl. Acoust. 121 (2017) 33–45.
[20] J. Singh, A.K. Darpe, S.P. Singh, Bearing damage assessment using Jensen-Rényi Divergence based on EEMD, Mech. Syst. Signal Process. 87 (2017) 307–339.
[21] L. Chen, Y.-Y. Zi, Z.-J. He, Y.-G. Lei, G.-S. Tang, Rotating machinery fault detection based on improved ensemble empirical mode decomposition, Adv. Adapt. Data Anal. 06 (2014) 1450006.
[22] J. Zhang, R. Yan, R.X. Gao, Z. Feng, Performance enhancement of ensemble empirical mode decomposition, Mech. Syst. Signal Process. 24 (2010) 2104–2123.
[23] W. Guo, P.W. Tse, A novel signal compression method based on optimal ensemble empirical mode decomposition for bearing vibration signals, J. Sound Vib. 332 (2013) 423–441.
[24] M. Kedadouche, M. Thomas, A. Tahan, A comparative study between empirical wavelet transforms and empirical mode decomposition methods: application to bearing defect diagnosis, Mech. Syst. Signal Process. 81 (2016) 88–107.
[25] J.-R. Yeh, J.-S. Shieh, N.E. Huang, Complementary ensemble empirical mode decomposition: a novel noise enhanced data analysis method, Adv. Adapt. Data Anal. 02 (2010) 135–156.
[26] X. Xue, J. Zhou, Y. Xu, W. Zhu, C. Li, An adaptively fast ensemble empirical mode decomposition method and its applications to rolling element bearing fault diagnosis, Mech. Syst. Signal Process. 62 (2015) 444–459.
[27] J. Zheng, Rolling bearing fault diagnosis based on partially ensemble empirical mode decomposition and variable predictive model-based class discrimination, Arch. Civ. Mech. Eng. 16 (2016) 784–794.
[28] M.E. Torres, M.A. Colominas, G. Schlotthauer, P. Flandrin, A complete ensemble empirical mode decomposition with adaptive noise, in: Proc. 36th IEEE Int. Conf. Acoust. Speech Signal Process., ICASSP 2011, Czech Republic, Prague, 2011: pp. 4144–4147.

[29] M.A. Colominas, G. Schlotthauer, M.E. Torres, Improved complete ensemble EMD: a suitable tool for biomedical signal processing, Biomed. Signal Process. Control. 14 (2014) 19–29.
[30] C. Sun, P. Wang, R. Yan, R.X. Gao, X. Chen, Machine health monitoring based on locally linear embedding with kernel sparse representation for neighborhood optimization, Mech. Syst. Signal Process. 114 (2019) 25–34.
[31] Y. Wang, G.H. Xu, L. Liang, K.S. Jiang, Detection of weak transient signals based on wavelet packet transform and manifold learning for rolling element bearing fault diagnosis, Mech. Syst. Signal Process. 54–55 (2015) 259–276.
[32] J. Wang, Q. He, Wavelet packet envelope manifold for fault diagnosis of rolling element bearings, IEEE Trans. Instrum. Meas. 65 (2016) 2515–2526.
[33] R. Yan, R.X. Gao, Rotary machine health diagnosis based on empirical mode decomposition, J. Vib. Acoust. 130 (2008) 021007.
[34] Y. Lei, M.J. Zuo, Fault diagnosis of rotating machinery using an improved HHT based on EEMD and sensitive IMFs, Meas. Sci. Technol. 20 (2009) 125701.
[35] H. Wang, J. Chen, G. Dong, Feature extraction of rolling bearing's early weak fault based on EEMD and tunable Q-factor wavelet transform, Mech. Syst. Signal Process. 48 (2014) 103–119.
[36] Y. Imaouchen, M. Kedadouche, R. Alkama, M. Thomas, A frequency-weighted energy operator and complementary ensemble empirical mode decomposition for bearing fault detection, Mech. Syst. Signal Process. 82 (2017) 103–116.
[37] D. Wang, Some further thoughts about spectral kurtosis, spectral L2/L1 norm, spectral smoothness index and spectral Gini index for characterizing repetitive transients, Mech. Syst. Signal Process. 108 (2018) 360–368.
[38] T. Barszcz, A. Jabłoński, A novel method for the optimal band selection for vibration signal demodulation and comparison with the Kurtogram, Mech. Syst. Signal Process. 25 (2011) 431–451.
[39] Z. Zhang, H. Zha, Principal manifolds and nonlinear dimensionality reduction via tangent space alignment, SIAM J. Sci. Comput. 26 (1) (2005) 313–338.
[40] J. Wang, Q. He, F. Kong, Automatic fault diagnosis of rotating machines by time-scale manifold ridge analysis, Mech. Syst. Signal Process. 40 (1) (2013) 237–256.
[41] H. Qiu, J. Lee, J. Lin, G. Yu, Wavelet filter-based weak signature detection method and its application on rolling element bearing prognostics, J. Sound Vib. 289 (2006) 1066–1090.